Dalton Transactions

PAPER

View Article Online
View Journal | View Issue

Cite this: *Dalton Trans.*, 2018, **47**, 4639

Greener synthesis of Cu-MOF-74 and its catalytic use for the generation of vanillin†

J. Gabriel Flores,‡[a,f] Elí Sánchez-González,‡[b] Aída Gutiérrez-Alejandre,[c] Julia Aguilar-Pliego,*[a,b] Ana Martínez,[d] Tamara Jurado-Vázquez,[b] Enrique Lima,[a,b] Eduardo González-Zamora,[e] Manuel Díaz-García,[f] Manuel Sánchez-Sánchez*[f] and Ilich A. Ibarra*[b]

Received 13th December 2017,
Accepted 19th February 2018

DOI: 10.1039/c7dt04701k

rsc.li/dalton

A greener synthesis of Cu-MOF-74 was obtained, for the first time, in methanol as the unique solvent and at room temperature. Full characterisation of the MOF material showed its purity and also its nanocrystalline nature. Complete activation (150 °C for 1 h and 10^{-3} bar) of Cu-MOF-74 afforded unsaturated Cu metal sites and this was corroborated by *in situ* DRIFT spectroscopy. The access to these Cu open metal sites was tested for the catalytic transformation of *trans*-ferulic acid to vanillin (yield of 71% and 97% selectivity) and a plausible catalytic reaction mechanism was postulated based on quantum chemical calculations.

Introduction

For at least a couple of decades there has been great emphasis on the development of clean and sustainable methodologies in research fields such as catalysis, organic synthesis and pharmacy. Comparatively, for the synthesis of metal–organic frameworks (MOFs) this progress has been significantly slower. MOFs are strongly proposed for different potential green applications but the lack of focus on their environmentally-friendly synthesis compromises their accreditation as 'green materials'. In addition, if MOFs are intended for industrial applications, their synthesis and processing must be scalable at relatively low pricing with high purity and yields. To date, the most common methodology to synthesise MOF materials is based on solvothermal batch reactions (long reaction times) quite often using toxic, carcinogenic and environmentally hazardous organic solvents. For example, dimethylformamide (DMF) is perhaps the most common organic solvent for MOF synthesis even though it is highly polluting, mutagenic and toxic.[1] DMF decomposes when heated at high temperatures for long periods (*e.g.* solvothermal reactions) and thus, cannot be reused.[2] Clearly, the replacement of such toxic solvents, with more benign alternatives,[3] is urgently needed for MOF synthesis. Another important parameter, which can considerably contribute to the sustainability of the synthetic process, is the reduction of the energy input as comprehensibly described by Friščić.[4] Room temperature synthesis is unquestionably the best alternative to completely minimize energy input. Some archetypal MOFs have been synthesised following this strategy at room temperature:[5a,b] HKUST-1 was synthesised from Cu$(OH)_2$ in a water ethanolic solution,[5c] ZIF-8 in a continuous flow system,[5d] and MIL-53 using the ligand sodium salt in water.[7b] Nonetheless, some of the room temperature syntheses could be improved by implementing a continuous flow system, a promising technology to scale up the MOF production.[6] This approach usually reports the nanometre size particles as a drawback, however, in the field of catalysis it plays a very important role by increasing the catalyst surface area. Our research group has previously taken advantage of room temperature synthetic approaches to fabricate MOF materials and in particular the M–MOF-74 family (M = Mn(II), Co(II), Ni(II), *etc.*).[7]

M$(DHTP)_2$, M–MOF-74 or CPO-27M is one of the most studied MOF materials due to its many interesting appli-

[a]*UAM-Azcapotzalco, San Pablo 180, Col. Reynosa-Tamaulipas, Azcapotzalco, C.P. 02200, Ciudad de México, Mexico*
[b]*Laboratorio de Fisicoquímica y Reactividad de Superficies (LaFReS), Instituto de Investigaciones en Materiales, Universidad Nacional Autónoma de México, Circuito Exterior s/n, CU, Del. Coyoacán, 04510 Ciudad de México, Mexico. E-mail: argel@unam.mx, apj@correo.azc.uam.mx; Fax: +52(55) 5622-4595*
[c]*UNICAT, Departamento de Ingeniería Química, Facultad de Química, Universidad Nacional Autónoma de México (UNAM), Coyoacán, C. P. 04510, Ciudad de México, Mexico*
[d]*Instituto de Investigaciones en Materiales, Universidad Nacional Autónoma de México, Circuito Exterior s/n, CU, Del. Coyoacán, 04510, Ciudad de México, Mexico*
[e]*Departamento de Química, Universidad Autónoma Metropolitana-Iztapalapa, San Rafael Atlixco 186, Col. Vicentina, Iztapalapa, C. P. 09340, Ciudad de México, Mexico*
[f]*Instituto de Catálisis y Petroleoquímica, ICP-CSIC, C/Marie Curie, 2 28049 Madrid, Spain. E-mail: manuel.sanchez@icp.csic.es*

†Electronic supplementary information (ESI) available: TGA data, ICP-MS data, NMR data, reaction mechanism, computational studies, SEM micrographs and EDS analysis. See DOI: 10.1039/C7DT04701K

‡These authors contributed equally to this work.

cations as demonstrated for gas capture,[8] separation[9] and heterogeneous catalysis.[10] Interestingly, this material has not been investigated for the catalytic conversion of *trans*-ferulic acid to vanillin.

We are interested in the generation of vanillin[11] since it is one of the most appreciated flavouring substances all around the world heavily used in different industries such as food, cosmetic, nutraceutical and pharmaceutical. Although vanillin can be extracted from natural sources (*Vanilla planifolia*), its worldwide production, by acid hydrolysis of lignin, corresponds to 99%. However, this chemical hydrolysis includes toxic solvents and strong oxidisers, which are very harmful to the environment. Although bio-processes are considerably more environmentally friendly, the drawback of long transformation waiting time, long purification and the potentially dangerous use of bacterial strains limit their applications.[12]

We report herein the greener synthesis of Cu-MOF-74 for the first time, to the best of our knowledge, using only methanol as a solvent and at room temperature. Full characterisation of the material, along with its application as a heterogeneous catalyst, for the oxidation of *trans*-ferulic acid to vanillin, under mild and environmentally compatible oxidation conditions was performed. Additionally, a new catalytic reaction mechanism as well as the possible structure degradation of the catalyst is proposed base on computation studies.

Experimental section

Synthetic preparations

A solution of 2,5-dihydroxyterephthalic acid (DHTP, 0.20 g, 1.0 mmol) in MeOH (6.67 g, 208 mmol) was added dropwise over a solution of $Cu(OAc)_2{\cdot}H_2O$ (0.40 g, 2.0 mmol) in MeOH (3.33 g, 104 mmol) for a period of 10 min with constant agitation and at room temperature. A precipitate containing Cu-MOF-74 as the only crystalline phase is formed. The agitation was continued for 20 h, at room temperature, after which the crystalline solid was recovered by centrifugation and washed with 10 mL of MeOH five times. The crystalline solid was kept immersed in 10 mL of MeOH for 6 days and exchanged for the same amount of fresh MeOH 3 times.

PXRD experiments

Powder X-ray diffraction (PXRD) data were collected under ambient conditions on a Bruker AXD D8 Advance diffractometer operated at 160 W (40 kV, 40 mA) for Cu Kα1 (λ = 1.5406 Å).

Scanning electron microscopy (SEM)

Morphology studies were carried out in an ultrahigh resolution Philips XL 30 SEM instrument with a tungsten filament.

TGA experiments

Thermal gravimetric analysis (TGA) was performed under N_2 at a heating rate of 2 °C min^{-1} using a TA Instruments Q500HR analyser.

Gas chromatography experiments

Gas chromatography (GC) was performed using a Carbowax column (25 m × 0.25 mm ID and 0.25 μm) with a He flow of 2.5 mL min^{-1}, FID 250 °C, heating ramps of 8 °C min^{-1} from 40 to 180 °C and of 10 °C min^{-1} from 180 to 210 °C.

Sorption isotherms for N_2

N_2 sorption isotherms (up to P/P_0 = 1 and 77 K) were performed on a Belsorp mini II analyser under vacuum (10^{-3} bar). Ultra-pure grade (99.9995%) N_2 was purchased from PRAXAIR. Samples of Cu-MOF-74 were activated at 150 °C for one hour (under 10^{-3} bar). N_2 adsorption isotherms for activated Cu-MOF-74, at 77 K, were performed to estimate a BET area ($0.01 < P/P_0 < 0.04$) of 1013 m^2 g^{-1} and a pore volume of 0.37 cm^3 g^{-1}.

DRIFT spectroscopy

DRIFT spectra of the catalytic material (Cu-MOF-74) were recorded using an FTIR Nicolet 6700 spectrophotometer (DTGS detector) with a 4 cm^{-1} resolution equipped with a diffuse reflectance vacuum chamber with KBr windows. DRIFT spectra were obtained on the as-synthesised Cu-MOF-74 sample (at room temperature), under vacuum (~6×10^{-3} Torr, 8×10^{-6} bar), and after increasing gradually the temperature up to 150 °C (*in situ* experiment).

Catalytic protocol

The activated catalyst (Cu-MOF-74: 150 °C for one hour and 10^{-3} bar), 0.05 g (6 mol%) suspended in EtOH (10 mL, all EtOH used here was previously degassed by bubbling N_2 for 5 min) was mixed with 5 mL of H_2O_2 (50 wt% in H_2O), 0.25 mL of acetonitrile and 0.50 g (2.57×10^{-3} mol) of *trans*-ferulic acid (dissolved in 20 mL of EtOH) under continuous stirring. 20 mL more of EtOH were added to the reaction mixture and heated to reflux for 4 h. In order to follow the catalytic reaction, an aliquot of 0.2 mL was taken every 30 min and its composition was analysed by column chromatography. After the reaction was complete, the catalyst was recovered by filtration; the filtrate was extracted with ethyl acetate and washed with a saturated solution of NH_4Cl. The combined organic phases were dried with anhydrous Na_2SO_4, filtered and concentrated under vacuum. Finally, the residue was purified by column chromatography (AcOEt–hexane 5 : 95).

Computational studies

Calculations associated with geometry optimisations were carried out by implementing Gaussian 09.[13] The geometry of the model was fully optimised at the B3LYP/LANL2DZ level.[14,15] Harmonic analyses were performed and local minima were identified (zero negative values).

Results and discussion

Characterisation of Cu-MOF-74

After the room temperature synthesis was complete (see synthetic preparations, Experimental section) the crystalline material (Cu-MOF-74) was first characterised by PXRD. Fig. 1 (top) shows the simulated and experimental PXRD patterns for Cu-MOF-74 where a good match is observed. The main characteristic of Cu-MOF-74 is the nanocrystalline nature covering the crystal size range from 35 to 50 nm, with a strong tendency to agglomerate as shown by SEM microscopy. Fig. 1 (bottom) shows a SEM micrograph of the as-synthesised Cu-MOF-74 nanocrystals where it is possible to observe, due to the crystal size, the agglomeration of the crystalline particles which were isolated after a mild sonication treatment. Thermogravimetric analysis (TGA, see Fig. S1, ESI†) confirmed the purity of the sample and the surface area of the activated catalyst (150 °C and 10^{-3} bar for 1 h) was measured using N_2 as a probe gas at 77 K. Application of the standard Brunauer–Emmett–Teller (BET) model to the adsorption data (P/P_0 = 0.05–0.3) afforded a measured surface area of 1013 $m^2\ g^{-1}$.

Activation of the catalyst (Cu-MOF-74)

The preparation of catalytically active MOFs[16] is quite often carried out using active (unsaturated) metals, which constitute a coordination network. Thus, the generation of vacant coordination sites on metal ions is normally achieved by the removal of labile ligands, commonly solvent molecules. Certainly, the generation of uncoordinated metal sites has been extensively focused on enhancing H_2 uptake in MOFs,[17] and remarkable examples have been presented for catalysis applications.[18] Apart from demonstrating the accessibility for uncoordinated metal sites, the retention of the crystallinity after the activation process is fundamental. Thus, we activated an as-synthesised sample of Cu-MOF-74 at 150 °C for 1 h and under vacuum (10^{-3} bar) to investigate the retention of the crystallinity by PXRD experiments. Fig. 2 shows the PXRD patterns of the as-synthesised Cu-MOF-74 and activated samples where the retention of the crystallinity of the material upon activation is clearly observed.

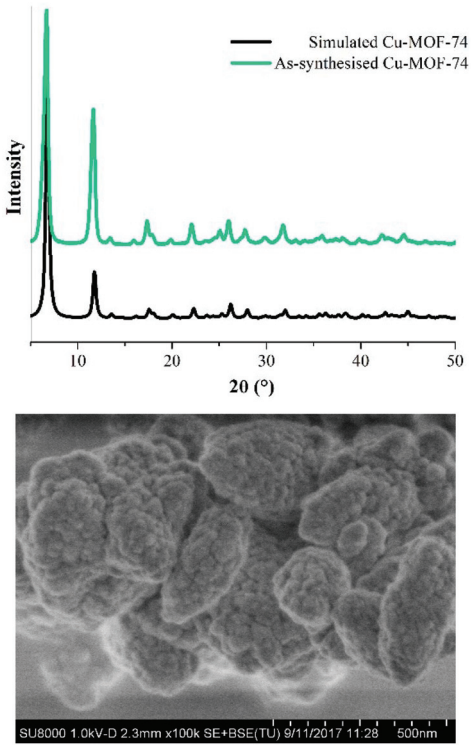

Fig. 1 (Top) PXRD patterns of the calculated (black) and as-synthesised (green) Cu-MOF-74; (Bottom) scanning electron micrograph of Cu-MOF-74.

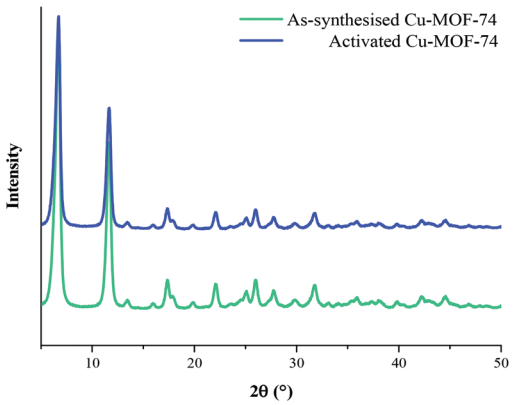

Fig. 2 PXRD patterns of the Cu-MOF-74 before and after the activation process.

Thus, it was demonstrated through PXRD experiments that the suggested activation conditions did not affect the crystalline structure of Cu-MOF-74. To establish whether the activation conditions removed the coordinated MeOH molecules (labile ligands) from the metal Cu(II) centres, *in situ* DRIFT experiments were carried out. A spectrum was recorded for the as-synthesised Cu-MOF-74 at 25 °C (room temperature), which is non-activated. After that, the cell-chamber was outgassed (~8×10^{-6} bar) at the same temperature, and a new spectrum was recorded. Under these conditions, the sample was heated, by the progressive increase of temperature, from room temperature to 150 °C; a decrease in the intensity of the band associated with coordinated MeOH to the Cu(II)-metal centre (1035 cm^{-1})[19a,b] was observed. This band, almost disappeared at 150 °C, indicating that the coordinated MeOH molecules to the Cu(II)-metal centre were removed as is shown in Fig. 3. In other words, the overall intensity of the FTIR spectra decreases when the temperature increases. However, the characteristic band (1035 cm^{-1}) corresponding to coordinated MeOH to the Cu(II) is completely lost from the spectra (at 150 °C), as previously reported.[19c]

Catalytic reaction

After experimentally demonstrating that the activation of the catalyst (Cu-MOF-74) did not affect its crystal structure (PXRD

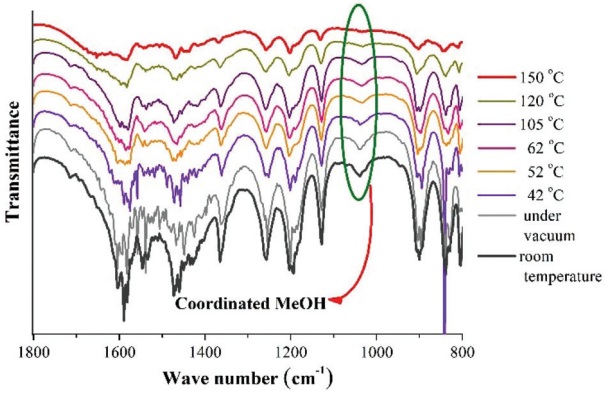

Fig. 3 *In situ* DRIFT spectra of Cu-MOF-74 at various temperatures under vacuum emphasising the transmission band attributed to coordinated MeOH.

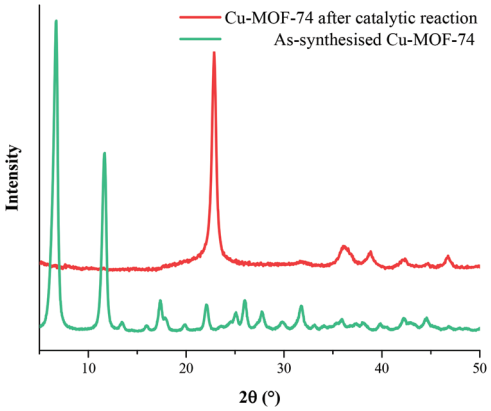

Fig. 5 PXRD patterns of the catalyst Cu-MOF-74 before and after the catalytic experiment.

experiments) and the possibility to gain access to the unsaturated Cu(II)-metal centres (DRIFT experiments), catalytic experiments were carried out (see Experimental). The selection of the oxidation of *trans*-ferulic acid to vanillin in this contribution was based on previous studies.[11] Fig. 4 shows the kinetics of the total yield of vanillin obtained from the oxidation of *trans*-ferulic acid using the activated catalyst Cu-MOF-74 and in the absence of any catalyst (blank experiment). When the catalytic reaction was complete (4 h), the reaction yield was equal to 71% and 97% vanillin selectivity was reached. The chemical composition of the reaction mixture was confirmed by GC analysis, and ^{1}H and ^{13}C NMR spectroscopy (see the ESI†). This reaction yield is comparable to the one obtained by Pagliaro and co-workers[20] and also by using an active Cu(II)-MOP.[11c] Furthermore, the use of a copper(II) salt as a catalyst in the oxidation of *trans*-ferulic acid was assayed by replacing Cu-MOF-74 for only $Cu(NO_3)_2$.[11] No conversion to vanillin was observed (Fig. 4).

After completing the catalytic reaction, the catalyst was recovered by filtration, washed with fresh ethanol and analysed

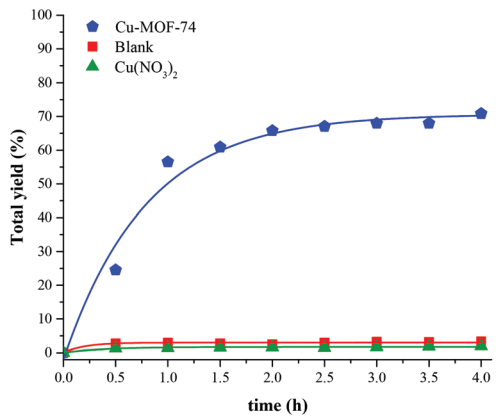

Fig. 4 Vanillin yields resulting from the oxidation of *trans*-ferulic acid in the presence of the activated catalyst Cu-MOF-74 and without a catalyst with H_2O_2 as a function of reaction time, and $Cu(NO_3)_2$ as a control.

by PXRD. Fig. 5 shows the PXRD patterns of the as-synthesised Cu-MOF-74 and the catalyst after the oxidation of *trans*-ferulic acid. Clearly, the crystallinity of the catalyst was partially lost affording a semi-amorphous material. For a heterogeneous catalyst it is important to keep its material integrity (*e.g.* crystalline structure) and none or no significant leaching of the catalytic active metal centre. Thus, inductively coupled plasma mass spectrometry (ICP-MS) was performed on a hot filtrate from the catalytic reaction, see the ESI.† The ICP-MS experiments revealed a Cu(II) leaching of 3.3 mg L^{-1}. We previously observed this relatively low chemical stability for Cu-MOF-74 in the oxidation of cyclohexene.[18h]

The crystalline phase was identified as copper(II) oxalate (see ESI, Fig. S4†), and it was formed *in situ.* As previously reported,[11] the *trans*-ferulic acid oxidation mechanism leads to the formation of glyoxylic acid as a by-product, which upon additional oxidation results in the formation of oxalic acid (for full mechanism see ESI, Scheme S1†). SEM analyses of the Cu-MOF-74 after the catalytic reaction showed the presence of two phases; one can be identified as the amorphous result of the MOF decomposition, the second are flower-like crystals radiating from an amorphous centre presumably copper oxalate (see ESI, Fig. S15†). Additionally, EDS analyses showed a homogeneous copper dispersion in both samples (see ESI, Fig. S16–7†), these reinforce our hypothesis of the Cu-MOF-74 partial decomposition and the growth of copper oxalate *in situ*.

A reaction mechanism for the catalytic transformation, considering the access to uncoordinated Cu(II) metal sites, has been previously proposed.[11] Thus, we have taken a simplified model (structure 1, see Fig. 6) to computationally describe such a catalytic mechanism (from *trans*-ferulic acid to vanillin): a Cu(II) metal centre, in a square planar geometry, connected to two carboxylate ligands (Fig. 6 and Scheme 1). In this model, geometry optimisations were performed.

Scheme 1 reports the optimised structures (from 1 to 9) of the models that were used in this investigation, according to the plausible reaction mechanism for the oxidation of *trans*-ferulic acid towards vanillin.[11] Then, the optimised structure 1

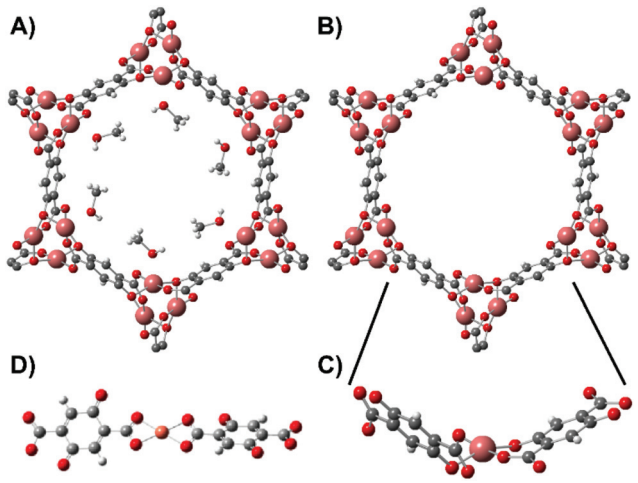

Fig. 6 Schematic representation of (A) the pore structure of Cu-MOF-74 showing the MeOH molecules inside the channel; (B) the pore structure free of MeOH molecules (as confirmed by *in situ* DRIFT); (C) section of the pore (model) that was taken to perform computational calculations and (D) the optimised structure of the model.

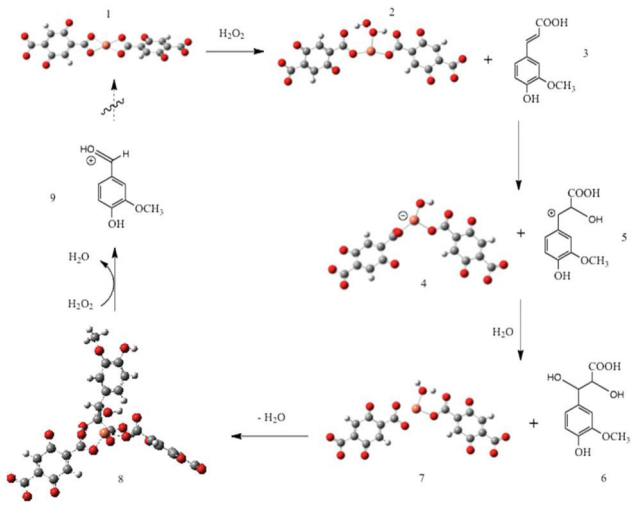

Scheme 1 Proposed reaction mechanism (*via* geometry optimisations) for the oxidation of *trans*-ferulic acid to vanillin.

(Scheme 1) is coordinated (nucleophilic attack) by H_2O_2 (2) and breaks two coordination bonds from the carboxylate functional groups to the Cu-metal centre. Structure 2 (see Scheme 1) is highly stabilised by relatively strong hydrogen bonds, forbidding the re-coordination of the carboxylate groups to the metal centre. Indeed, structure 2 is the most interesting of the catalytic cycle since it entails the activation of the Cu centres to react in contact with *trans*-ferulic acid (3), pushing forward the catalytic transformation. Additionally, structure 2 explains why Cu(II) ions were leached out after the catalytic reaction: H_2O_2 is able to partially destroy the square planar geometry around Cu(II), and at the same time (*via* hydrogen bonding) to stabilise these metal centres to perform

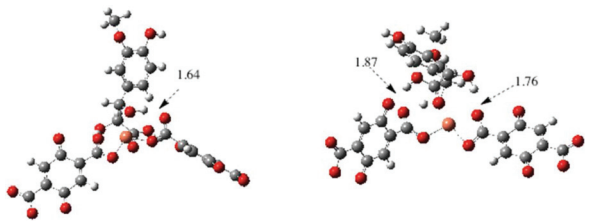

Fig. 7 Two different views of the optimised structure 8 emphasising the intramolecular hydrogen bond lengths.

the catalytic reaction. However, once some coordination bonds were lost (due to the addition of H_2O_2), the overall crystallinity of Cu-MOF-74 was also lost and some leaching of the Cu(II) ions was observed. In other words, the addition of H_2O_2 promotes (i) the catalytic transformation and (ii) the partial decomposition of Cu-MOF-74.

Interestingly, all the structures (from 2 to 8, Scheme 1) showed intramolecular hydrogen bonds (see the ESI†) which contributed to the stabilisation of the catalytic transformation, but also broke the coordination bonds around the catalytic metal centre and for this reason, the reaction did not continue up to 1 (see Scheme 1).

For example, Fig. 7 shows the optimised structure of structure 8 (intramolecular hydrogen bonds are indicated), where it is clearly observed that these hydrogen bonds promote the dissociation of two of the Cu–O bonds and the catalytic Cu(II) centre is modified.

Conclusions

A greener synthesis of Cu-MOF-74 was successfully achieved, for the first time to the best of our knowledge, in only methanol at room temperature. PXRD, BET and TGA analyses confirmed its purity and SEM microscopy showed the nanocrystalline nature of the synthesised material (crystal size from 35 to 50 nm). Access to the uncoordinated Cu(II) metal sites, within Cu-MOF-74, by thermal activation was demonstrated by *in situ* DRIFT experiments. PXRD data showed the retention of the crystallinity of the MOF material after the activation conditions. Activated Cu-MOF-74 was used as a heterogeneous catalyst for the transformation of *trans*-ferulic acid to vanillin, giving a reaction yield of 71% and 97% vanillin selectivity. The recovered catalyst was analysed by PXRD showing the phase transformation of Cu-MOF-74, and ICP-MS experiments confirmed the certain leaching of Cu(II), 3.3 mg L^{-1}. Geometry optimisations corroborated the proposed reaction mechanism and, more importantly, explained the relatively low chemical stability of Cu-MOF-74 under the reaction conditions. Our proposed optimised model (Cu(II) in a square planar geometry connected to two carboxylate ligands) showed how upon coordination of H_2O_2, the dissociation of two Cu–O bonds occurred and although the catalytic reaction proceeded, the disruption on the framework structure was irreversible, trans-

formed into copper oxalate. Currently, our research group is investigating the use of different (softer) organic bases in order to catalytically convert *trans*-ferulic acid to vanillin and to preserve the material integrity of Cu-MOF-74.

Conflicts of interest

There are no conflicts to declare.

Acknowledgements

The authors thank Dr A. Tejeda-Cruz (X-ray; IIM-UNAM), Dr O. Novelo-Peralta (SEM; IIM-UNAM), PAPIIT UNAM Mexico (IN101517) and CONACyT (1789) for financial support. E. G.-Z. thanks CONACyT (236879), Mexico for financial support. This work has been partially financed by the Spanish State Research Agency (AEI) and the European Regional Development Fund (FEDER) through the Project MAT2016-77496-R (AEI/FEDER, UE). Thanks to U. Winnberg (ITAM) for scientific discussions. Computational calculations were carried out using a NES supercomputer, provided by Dirección General de Cómputo y Tecnologías de Información y Comunicación (DGTIC), Universidad Nacional Autónoma de México (UNAM).

Notes and references

1 R. P. Pohanish, *Sittig's Handbook of Toxic and Hazardous Chemicals and Carcinogens*, William Andrew Publishing, 5th edn, 2008.
2 M. A. Grela, V. T. Amorebieta and A. J. Colussi, *J. Phys. Chem.*, 1985, **89**, 38.
3 (*a*) I. A. Ibarra, P. A. Bayliss, E. Pérez, S. Yang, A. J. Blake, H. Nowell, D. R. Allan, M. Poliakoff and M. Schöder, *Green Chem.*, 2012, **14**, 117; (*b*) P. A. Bayliss, I. A. Ibarra, E. Pérez, S. Yang, C. C. Tang, P. Martyn and S. Martin, *Green Chem.*, 2014, **16**, 3796.
4 P. A. Julien, C. Mottillo and T. Friščić, *Green Chem.*, 2017, **19**, 2729.
5 (*a*) H. Reinsch, *Eur. J. Inorg. Chem.*, 2016, 4290; (*b*) J. Chen, K. Shen and Y. Li, *ChemSusChem*, 2017, **10**, 3165; (*c*) G. Majano and J. Pérez-Ramírez, *Adv. Mater.*, 2013, **25**, 1052; (*d*) A. Polyzoidis, T. Altenburg, M. Schwarzer, S. Loebbecke and S. Kaskel, *Chem. Eng. J.*, 2016, **283**, 971.
6 (*a*) M. Rubio-Martinez, C. Avci-Camur, A. W. Thornton, I. Imaz, D. Maspochbc and M. R. Hill, *Chem. Soc. Rev.*, 2017, **46**, 3453; (*b*) J. Ren, X. Dyosiba, N. M. Musyoka, H. W. Langmi, M. Mathe and S. Liao, *Coord. Chem. Rev.*, 2017, **352**, 187.
7 (*a*) M. Díaz-García, A. Mayoral, I. Díaz and M. Sánchez-Sánchez, *Cryst. Growth Des.*, 2014, **14**, 2479; (*b*) M. Sánchez-Sánchez, N. Getachew, K. Díaz, M. Díaz-García, Y. Chebude and I. Díaz, *Green Chem.*, 2015, **17**, 1500; (*c*) N. Getachew, Y. Chebude, I. Díaz and M. Sánchez-Sánchez, *J. Porous Mater.*, 2014, **21**, 769; (*d*) M. Sanchez-Sanchez, I. de Asua, D. Ruano and K. Diaz, *Cryst. Growth Des.*, 2015, **15**, 4498; (*e*) K. Guesh, C. A. D. Caiuby, Á. Mayoral, M. Díaz-García, I. Díaz and M. Sanchez-Sanchez, *Cryst. Growth Des.*, 2017, **17**, 1806.
8 G. Orcajo, G. Calleja, J. A. Botas, L. Wojtas, M. H. Alkordi and M. Sánchez-Sánchez, *Cryst. Growth Des.*, 2014, **14**, 739.
9 J. A. Botas, G. Calleja, M. Sánchez-Sánchez and M. G. Orcajo, *Int. J. Hydrogen Energy*, 2011, **36**, 10834.
10 P. Leo, G. Orcajo, D. Briones, G. Calleja, M. Sánchez-Sánchez and F. Martínez, *Nanomaterials*, 2017, **7**, 149.
11 (*a*) R. Yepez, S. García, P. Schachat, M. Sánchez-Sánchez, J. H. González-Estefan, E. González-Zamora, I. A. Ibarra and J. Aguilar-Pliego, *New J. Chem.*, 2015, **39**, 5112; (*b*) R. Yepez, J. F. Illescas, P. Gijón, M. Sánchez-Sánchez, E. González-Zamora, R. Santillan, J. R. Álvarez, I. A. Ibarra and J. Aguilar-Pliego, *J. Visualized Exp.*, 2016, **113**, e54054; (*c*) E. Sánchez-González, A. López-Olvera, O. Monroy, J. Aguilar-Pliego, J. G. Flores, A. Islas-Jácome, M. A. Rincón-Guevara, E. González-Zamora, B. Rodríguez-Molina and I. A. Ibarra, *CrystEngComm*, 2017, **19**, 4142.
12 (*a*) N. J. Walton, M. J. Mayer and A. Narbad, *Phytochemistry*, 2003, **63**, 505; (*b*) S. Serra, C. Fuganti and E. Brenna, *Trends Biotechnol.*, 2005, **23**, 193.
13 M. J. Frisch, G. W. Trucks, H. B. Schlegel, G. E. Scuseria, M. A. Robb, J. R. Cheeseman, G. Scalmani, V. Barone, B. Mennucci, G. A. Petersson, H. Nakatsuji, M. Caricato, X. Li, H. P. Hratchian, A. F. Izmaylov, J. Bloino, G. Zheng, J. L. Sonnenberg, M. Hada, M. Ehara, K. Toyota, R. Fukuda, J. Hasegawa, M. Ishida, T. Nakajima, Y. Honda, O. Kitao, H. Nakai, T. Vreven, J. A. Montgomery Jr., J. E. Peralta, F. Ogliaro, M. Bearpark, J. J. Heyd, E. Brothers, K. N. Kudin, V. N. Staroverov, R. Kobayashi, J. Normand, K. Raghavachari, A. Rendell, J. C. Burant, S. S. Iyengar, J. Tomasi, M. Cossi, N. Rega, J. M. Millam, M. Klene, J. E. Knox, J. B. Cross, V. Bakken, C. Adamo, J. Jaramillo, R. Gomperts, R. E. Stratmann, O. Yazyev, A. J. Austin, R. Cammi, C. Pomelli, J. W. Ochterski, R. L. Martin, K. Morokuma, V. G. Zakrzewski, G. A. Voth, P. Salvador, J. J. Dannenberg, S. Dapprich, A. D. Daniels, Ö. Farkas, J. B. Foresman, J. V. Ortiz, J. Cioslowski and D. J. Fox, *Gaussian 09, (Revision A.08)*, Gaussian, Inc., Wallingford CT, 2009.
14 (*a*) A. D. Becke, *J. Chem. Phys.*, 1993, **98**, 5648; (*b*) C. Lee, W. Yang and R. G. Parr, *Phys. Rev. B: Condens. Matter Mater. Phys.*, 1988, **37**, 785; (*c*) B. Miehlich, A. Savin, H. Stoll and H. Preuss, *Chem. Phys. Lett.*, 1989, **157**, 200.
15 (*a*) P. J. Hay and W. R. Wadt, *J. Chem. Phys.*, 1985, **82**, 270; (*b*) P. J. Hay and W. R. Wadt, *J. Chem. Phys.*, 1985, **82**, 299; (*c*) W. R. Wadt and P. J. Hay, *J. Chem. Phys.*, 1985, **82**, 284.
16 (*a*) S. S. Y. Chui, S. M. F. Lo, J. P. H. Charmant, A. G. Orpen and I. D. Williams, *Science*, 1999, **283**, 1148; (*b*) O. K. Farha, A. M. Shultz, A. A. Sarjeant, S. T. Nguyen and J. T. Hupp, *J. Am. Chem. Soc.*, 2011, **133**, 5652; (*c*) J.-P. Zhang, S. Horike and S. Kitagawa, *Angew. Chem., Int. Ed.*, 2007, **46**, 889; (*d*) Z. Wang and S. M. Cohen, *Chem. Soc. Rev.*, 2009, **38**,

1315; (*e*) P. Falcaro, R. Ricco, A. Yazdi, I. Imaz, S. Furukawa, D. Maspoch, R. Ameloot, J. D. Evans and C. J. Doonan, *Coord. Chem. Rev.*, 2016, **307**, 237; (*f*) J. D. Evans, C. J. Sumby and C. J. Doonan, *Chem. Soc. Rev.*, 2014, **43**, 5933.

17 (*a*) M. Dincă and J. R. Long, *Angew. Chem., Int. Ed.*, 2008, **47**, 6766–6679; (*b*) I. A. Ibarra, X. Lin, S. Yang, A. J. Blake, G. S. Walker, S. A. Barnett, D. R. Allan, N. R. Champness, P. Hubberstey and M. Schröder, *Chem. – Eur. J.*, 2010, **16**, 13671.

18 (*a*) M. Gustafsson, A. Bartoszewicz, B. Martín-Matute, J. Sun, J. Grins, T. Zhao, Z. Li, G. Zhu and X. Zou, *Chem. Mater.*, 2010, **22**, 3316; (*b*) L. Mitchell, B. Gonzalez-Santiago, J. P. S. Mowat, M. E. Gunn, P. Williamson, N. Acerbi, M. L. Clarke and P. A. Wright, *Catal. Sci. Technol.*, 2013, **3**, 606; (*c*) K. S. Jeong, Y. B. Go, S. J. Lee, J. Kim, O. M. Yaghi and N. Jeong, *Chem. Sci.*, 2011, **2**, 877; (*d*) A. Henschel, K. Gedrich, R. Kraehnert and S. Kaskel, *Chem. Commun.*, 2008, 4192; (*e*) A. Dhakshinamoorthy, M. Alvaro, H. Chevreau, P. Horcajada, T. Devic, C. Serre and H. Garcia, *Catal. Sci. Technol.*, 2012, **2**, 324; (*f*) L. Kurfirtova, Y.-K. Seo, Y. K. Hwang, J.-S. Chang and J. Cejka, *Catal. Today*, 2012, **179**, 85; (*g*) M. J. Beier, W. Kleist, M. T. Wharmby, R. Kissner, B. Kimmerle, P. A. Wright, J.-D. Grunwaldt and A. Baiker, *Chem. – Eur. J.*, 2012, **18**, 887; (*h*) D. Ruano, M. Díaz-García, A. Alfayate and M. Sanchez-Sanchez, *ChemCatChem*, 2015, **7**, 674.

19 (*a*) J. A. Villajos, G. Orcajo, C. Martos, J. A. Botas, J. Villacañas and G. Calleja, *Int. J. Hydrogen Energy*, 2015, **40**, 5346; (*b*) M. Dincă, W. S. Han, Y. Liu, A. Dailly, C. M. Brown and J. R. Long, *Angew. Chem., Int. Ed.*, 2007, **46**, 1419; (*c*) I. A. Ibarra, X. Lin, S. Yang, A. J. Blake, G. S. Walker, S. A. Barnett, D. R. Allan, N. R. Champness, P. Hubberstey and M. Schröder, *Chem. – Eur. J.*, 2010, **16**, 13671.

20 R. Delisi, R. Ciriminna, F. Parrino, L. Palmisano, Y.-J. Xu and M. Pagliaro, *ChemistrySelect*, 2016, **3**, 626.